Materials Science & Engineering C 119 (2021) 111539

Contents lists available at ScienceDirect

Materials Science & Engineering C

journal homepage: www.elsevier.com/locate/msec

Functionalised peptide hydrogel for the delivery of cardiac progenitor cells

K.A. Burgess[a,b], C. Frati[c], K. Meade[a], J. Gao[a,b], L. Castillo Diaz[a,b,1], D. Madeddu[c], G. Graiani[c], S. Cavalli[c], A.F. Miller[b,d,2], D. Oceandy[e], F. Quaini[c], A. Saiani[a,b,*]

[a] Department of Materials, The University of Manchester, Oxford Road, Manchester M13 9PL, UK
[b] Manchester Institute of Biotechnology, The University of Manchester, Oxford Road, Manchester M13 9PL, UK
[c] Department of Medicine and Surgery, University of Parma, Italy
[d] Department of Chemical Engineering and Analytical Sciences, The University of Manchester, Oxford Road, Manchester M13 9PL, UK
[e] Division of Cardiovascular Sciences, The University of Manchester, Oxford Road, Manchester M13 9PL, UK

ARTICLE INFO

Keywords:
Hydrogel
Injectable
Peptide
Self-assembly
Cardiac repair
Cell culture

ABSTRACT

Heart failure (HF) remains one of the leading causes of death worldwide; most commonly developing after myocardial infarction (MI). Since adult cardiomyocytes characteristically do not proliferate, cells lost during MI are not replaced. As a result, the heart has a limited regenerative capacity. There is, therefore, a need to develop novel cell-based therapies to promote the regeneration of the heart after MI. The delivery and retention of cells at the injury site remains a significant challenge. In this context, we explored the potential of using an injectable, RGDSP-functionalised self-assembling peptide — FEFEFKFK — hydrogel as scaffold for the delivery and retention of rat cardiac progenitor cells (CPCs) into the heart. Our results show that culturing CPCs in vitro within the hydrogel for one-week promoted their spontaneous differentiation towards adult cardiac phenotypes. Injection of the hydrogel on its own, or loaded with CPCs, into the rat after injury resulted in a significant reduction in myocardial damage and left ventricular dilation.

1. Introduction

Heart failure (HF) remains one of the leading causes of death worldwide; most commonly developing after myocardial infarction (MI) [1]. Even though the prevalence of HF has remained relatively stable over the last decade, the absolute number of cases and thus its burden on national health services is ever-increasing [2]. Since adult cardiomyocytes turnover is characteristically low, cells lost during MI are not replaced. As a result, the heart has a limited regenerative capacity (≤1% replaced annually) [3] and tissue lost during MI is replaced by a non-contractile fibrotic scar, which in turn, propagates a cyclic cascade of detrimental remodelling [4]. Currently, heart transplantation remains the only curative treatment. However, transplantation is not always possible owing to donor shortages and patient-ineligibility [5]. There is, therefore, an increasing need for the development of cell-based therapies to promote regeneration of the heart after MI.

The use of stem cells as an intervention therapy was first conceptualised more than 15 years ago; yet to date, such bio-interventions have failed to gain approval for clinical use [6]. Over the years, multiple clinical trials — utilising several cell types (e.g. bone marrow-derived progenitor cells, mesenchymal stem cells and cardiac progenitor cells) — have shown that these therapies are well-tolerated with regards to safety but failed to show any significant improvement in efficacy outcomes [7]. The main reasons for failure are thought to be: poor retention of exogenous cells at the delivery site; extremely low implantation efficiency (< 1–2%); and, as far as heart regeneration is concerned, lack of suitable stem cell phenotypes that differentiate into functional cardiomyocytes [6]. The advent of induced pluripotent stem cells (iPSC) has improved the availability of cells for cardiac transplantation [8], indeed iPSC-derived cardiac progenitor cells (CPC) have recently been shown to be both proliferative and committed to differentiate towards cardiac lineages [9]. In a recent study, iPSC-derived CPCs were allowed — after delivery into the heart — to first proliferate before inducing differentiation towards cardiac lineages, a strategy which resulted in improved tissue regeneration and functional outcomes in a mouse MI model [10]. However, the issue of cell retention and survival at delivery site still remains a challenge for such therapies.

There is currently a significant amount of research focusing on the design of translatable injectable scaffolds for the delivery of cells to

* Corresponding author at: Department of Materials, The University of Manchester, Oxford Road, Manchester M13 9PL, UK.
E-mail address: a.saiani@manchester.ac.uk (A. Saiani).
[1] Current address: Departamento de Medicina y Ciencias de la Salud, División de Ciencias Biológicas y de la Salud, Universidad de Sonora, Hermosillo, Mexico.
[2] Current address: Manchester BIOGEL, 19F4 Mereside, Alderley Park, Alderley Edge, Cheshire SK10 4TG, UK.

https://doi.org/10.1016/j.msec.2020.111539
Received 9 July 2020; Received in revised form 5 September 2020; Accepted 16 September 2020
Available online 22 September 2020

improve their retention and implantation [11–13]. Self-assembling peptide hydrogels have attracted significant interest due to their excellent biocompatibility, low immunogenicity [14,15], and unique shear thinning and recovery properties. In addition, short self-assembling peptides allow overcoming some of the limitations encountered with both natural and synthetic polymers. They are chemically fully defined and easy to synthesise, and therefore functionalise, and purify through standard processes, which is not always the case for natural polymers such as proteins and being build form natural amino acids they can be degraded and metabolised by the body, which is not always the case for synthetic polymers. A variety of short peptide designs can be found in the literature, which self-assemble and above a critical gelation concentration (CGC) entangle/associate to form 3D networks and hydrogels [16,17]. As far as gelation is concerned β-sheet forming peptides have been shown to allow the formulation of highly stable hydrogels, with physical and functional properties that can be easily tailored by design [18–20] to the targeted application [21–23]. These highly hydrated materials have a nanofibrillar structure that mimics the extracellular matrix and have been shown to allow not only the 3D-culture of a variety of cell lines [24–29] but also the differentiation of stem cells [30–32].

In the present work, we decided to investigate the potential use of a self-assembling octa-peptide hydrogel developed by our group and based on the design first proposed by Zhang and co-workers, alternation of hydrophilic and hydrophobic residues, for the delivery of CPCs to the heart using a rat MI model. The self-assembling and gelation properties of FEFEFKFK (F: phenylalanine; E: glutamic acid; K: lysine) peptide were first investigated by Caplan at al [33–35]. These authors showed that this peptide readily self-assembles into anti-parallel β-sheets and forms stable and transparent hydrogels above the CGC: ~5 mg mL^{-1} at pH 7 [24]. We recently showed that FEFEFKFK hydrogels could be used for 3D cell culture of chondrocytes [24], osteoblasts [25] and nucleus pulposus cells [36], as well as for the directed differentiation of mesenchymal stem cells towards osteoblast lineage [37]. One interesting property of this peptide, which is linked to its design, is the change in hydrogel mechanical properties upon addition of cell culture media. At pH 4 and 9, FEFEFKFK carries a +2 and −2 charge respectively and strong electrostatic repulsion interactions between peptide fibres counterbalance the hydrophobic attractive interactions resulting in a low number of weak network crosslinks forming, leading to weak, shear-thinning hydrogels with shear storage moduli (G′) in the range of 0.1 to 1 kPa, depending on peptide concentration and exact pH. Once cell culture media is added and the hydrogel pH is changed to 7.4, FEFEFKFK carries no overall net charge and the hydrophobic attractive interactions between fibres become dominant resulting in the formation of an increased number of strong network crosslinks, leading to the formation of strong, brittle hydrogels with G′ one order of magnitude larger, ranging from 5 to 20 kPa. This property makes the hydrogel easy to handle before addition of the media and allows after media addition to obtain mechanical properties similar to a range of human tissues [38]. To improve cell adhesion to the hydrogel scaffold, we also decided to functionalise the hydrogel using the well-established cell-adhesion motif RGD (R: arginine; G: glycine; D: aspartic acid) which is found across a variety of ECM proteins [39–42]. For this purpose, the functionalised peptide RGDSP-FEFEFKFK (S: serine; P: proline) was purchased and doped (30% wt.) into the hydrogel formulation to create functional hydrogels as schematically shown in Fig. 1.

2. Materials and methods

2.1. Rat cardiac progenitor cells (CPCs) isolation

CPCs were isolated from transgenic green fluorescence protein positive ($EGFP^{pos}$) [27] and wild type rats and cultured as previously described [28].

In this study CPCs at passage 3 and 4 (P3–P4) were employed.

2.2. Hydrogel formulation

Peptide hydrogels were prepared to a final concentration of 10 mg mL^{-1} (~ 90% water content by volume), using a method described previously [37]. Briefly, the required lyophilised peptide powder (HCl salt; > 95% purity) (BioMatik, Wilmington, DE) was dissolved in HPLC grade water and the pH adjusted to 9 using a 0.5 M NaOH (Merck, Italy) solution. The sample was vortexed vigorously between each NaOH addition. Once pH 9 was reached the sample were placed in an oven at 90 °C for 2 h to ensure full homogenisation. Upon cooling to room temperature (~2–5 min), the sample formed a weak transparent hydrogel. Functionalised and fluorescent hydrogels were obtained by mixing the peptide powders first, before preparing the hydrogels as described above. The relative weight ratios were as follows: FEFEFKFK/RGDSP-FEFEFKFK: 70/30 and FEFEFKFK/MCA-FEFEFKFK: 50/50, respectively.

2.3. Cell culture

In order to study the hydrogel's ability of supporting cell culture and the effects of RGDSP functionalisation on progenitor cell differentiation, $EGFP^{pos}$ and wild type CPCs were cultured using a 3D "sandwich culture" approach. Briefly, a layer of FEFEFKFK or RGDSP-FEFEFKFK hydrogel (500 μl) was plated in a chamber slide (Falcon, USA) and left to set. Next, a solution of CPCs (100 μl; 1.5×10^5 cells mL^{-1}) was seeded onto the hydrogel. The CPCs were then covered by a second layer of hydrogel and incubated with media. Media was replaced every other day. After 6 days, encapsulated $EGFP^{pos}$ CPCs were observed and analyzed using an inverted microscope (Axiovert 200M, Carl Zeiss, Jena, Germany), integrated with the confocal system (LSM 510 Meta scan head). The resultant stacks were rendered in 3D using the AxioVision© (Carl Zeiss Imaging Solutions) software.

2.4. Cell Rescue and immunocytochemistry

After 7 days of culture, FEFEFKFK or RGDSP-FEFEFKFK hydrogels were washed twice with PBS, centrifuged at 1100 rpm for 5 min and the pellet re-plated in chamber slides. After several hours, surviving wild type CPCs had adhered to the surface and media containing suspended hydrogel fragments was replaced with fresh media. Surviving CPCs were maintained in culture for up to 3 weeks. After 2 weeks, immunocytochemical analysis was performed for markers of myocardial adult phenotypes. Briefly, cells were fixed in 4% paraformaldehyde for 1 h at room temperature. Samples were blocked with serum and incubated with primary antibodies against α-smooth muscle actin (α-SMA: mouse monoclonal; Merck, Italy) and α-sarcomeric actin (α-SARC: mouse monoclonal; Merck, Italy). Cells were subsequently stained with FITC-conjugated secondary antibody (Merck, Italy). Cell nuclei were imaged using DAPI (4′,6-diamidine-2-phenyndole, Merck, Italy).

2.5. In vivo study

The study population consisted of male Wistar rats (*Rattus norvegicus*, Charles River, Italy) bred at the University of Parma departmental animal facility, weighing 230–280 g (BW). The investigation was approved by the Veterinary Animal Care and Use Committee of the University of Parma and conformed to the National Ethical Guidelines (Italian Ministry of Health; D.L.vo 116, January 27, 1992) and the Guide for the Care and Use of Laboratory Animals (NIH publication no. 85–23, revised 1996). To assess peptide hydrogel (10 mg mL^{-1}) injectability, 300 μl of hydrogels with rhodamine particles (F8826, Thermofisher, Italy) were injected into the myocardium of a healthy rat heart (N = 3). Rhodamine particles were mixed directly into the hydrogel using the tip of a pipette and directly visualised by UV excitation of tissue sections. To document peptide hydrogel cell retention

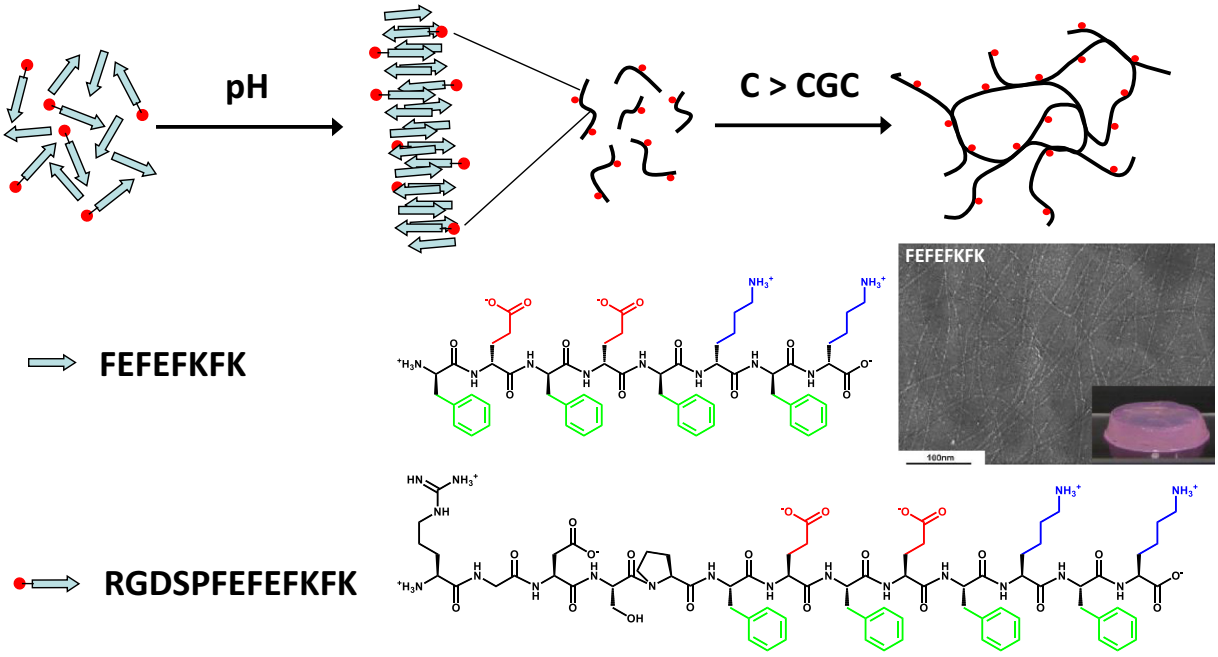

Fig. 1. Schematic representation of the self-assembly and gelation pathway of the peptide, chemical structure of the peptides and TEM image of FEFEFKFK fibres (inset: photograph of hydrogel after cell culture media addition).

Quantum Dots-labelled CPCs (QDots, Invitrogen) mixed into fluorescent hydrogel were injected into the myocardium of a healthy rat heart (N = 3). In addition, to test the in vivo properties of peptide hydrogels, further experiments were performed on rat models of cryoinjury (CI) and myocardial infarction (MI).

2.6. Surgical procedure

Myocardial damage was induced using either cryoinjury (CI) [30] or myocardial infarction (MI) model [43]. Following CI or MI injury, RGDSP-FEFEFKFK hydrogel (10 mg mL^{-1}) was injected (3 injections of 30 μl each) with (+CPCs) or without rat $EGFP^{pos}$ CPCs (3×10^5 cells mL^{-1}) into the border zone of the damaged area of the rat heart. Control groups (CTRL) were represented by animals subjected to myocardial damage without injection. The numbers of animals employed in each experimental group are detailed in Table ESI 1. Rats were then sacrificed at 4 and 10 days after CI and 30 days after MI; chest was opened, and the heart arrested in diastole and perfused with 4% buffered formalin.

2.7. Cardiac anatomy

The heart was excised and fixed for 24 h in 4% formalin, and the right ventricle (RV) and the left ventricle (LV) were separated and weighed. LV chamber volume was calculated according to the Dodge equation, which equalizes the ventricular cavity to an ellipsoid [44]. Subsequently, the LV was sliced in 3 mm thick transverse sections and the equatorial portion was embedded in paraffin. Five-μm-thick sections were cut for morphometric and immunohistochemical studies [30].

2.8. Histologic and immunohistochemical analysis

Heart sections from all experimental groups were stained with haematoxylin and eosin (H&E) and Masson's trichrome to analyze tissue composition and to detect the site of injection. The presence of injected $EGFP^{pos}$ CPCs within myocardial tissue and the differentiation of progenitor cells towards cardiomyogenic phenotypes were determined by immunohistochemistry. EGFP and α-sarcomeric actin (α-SARC) were detected by immunofluorescence. To this purpose, LV sections from different experimental groups were incubated with primary antibodies (polyclonal goat anti-GFP (ab6673), dilution 1:100, Abcam and monoclonal mouse anti-α-SARC (A2172), dilution 1:100, Merck). FITC- or TRITC-conjugated specific secondary antibodies were used to detect the epitope. Nuclei were recognized by the blue fluorescence of DAPI staining.

2.9. Statistical analysis

The SPSS statistical package was used (SPSS, Chicago, IL, USA). Statistics of variables included mean ± standard error (SEM), paired Student *t*-test, and one-way analysis of variance (ANOVA, post-hoc analyses: Tukey test or Holm–Sidak test, when appropriate). Statistical significance was set at $p < 0.05$.

3. Results and discussion

As stated above, self-assembling peptide hydrogels have unique shear-thinning and recovery properties which makes them ideal injectable scaffolds. In Fig. 2A, the rheological properties of FEFEFKFK hydrogel were explored using oscillatory shear rheometry. First a low shear strain (1%) within the linear viscoelastic region of the material was applied. As can be seen, a solid-like behaviour characteristic of hydrogels was observed with a storage shear modulus G′ (~ 1 kPa) one order of magnitude larger than the loss shear modulus G″ (~80 Pa). Both G′ and G″ were found to be constant over time showing the formation of a stable hydrogel. After 5 min the shear strain was increased to 150%, above the yield shear strain of the material, to simulate the shear stresses applied during injection. The hydrogel was found to shear-thin ("liquefy") within a few seconds and G′ and G″ decreased with G′ becoming one order of magnitude smaller than G″, which is characteristic of a liquid-like behaviour. After 1 min, the low shear strain was restored and G′ and G″ recovered within a few seconds to their original values, indicating that the sample "re-gelled" very quickly. The shear-thinning and recovery properties of this family of peptides have been the subject of several detailed studies recently

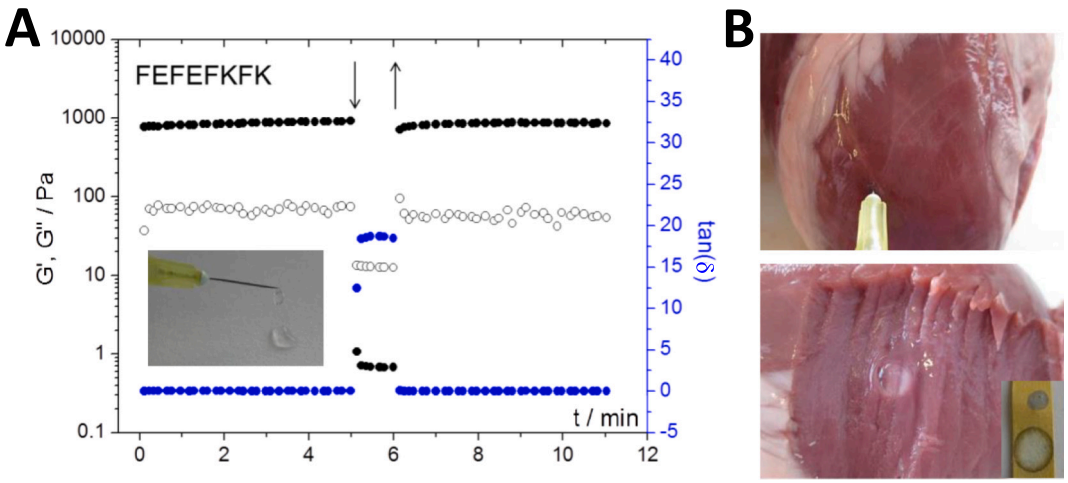

Fig. 2. A) Shear thinning and recovery behaviour of FEFEFKFK hydrogel (G′: storage shear modulus; G″: shear loss modulus and tan δ = G″ / G′). Experiments were performed at 1 Hz and shear strain of 1% (0–5 min and 6-11 min) and 150% (5–6 min; arrow down shows application and arrow up shows removal of high shear strain) were applied alternatingly. B) Photograph of hydrogel being injected in lamb heart (top) and of hydrogel after injection in lamb heart (bottom); inset: photograph of hydrogels on yellow litmus paper before (bottom) and after (top) injection. (For interpretation of the references to color in this figure legend, the reader is referred to the web version of this article.)

[20,45,46]. The common thinking is that when sheared these hydrogels, due to their self-assembled nature, break into micron-size domains that slide and tumble over each other, resulting in the apparent liquid-like behaviour observed above. When the high shear strain is removed, the hydrogels recover their original bulk properties very quickly due to the fast re-assembly and re-organization dynamics of this family of peptides and the fibres they form.

To visualise the injection of the material into a heart, a 27-gauge needle was used to inject the hydrogel into a lamb heart ex vivo. The injection was performed by keeping the needle steady in order to inject all of the hydrogel at the same location. After 15 min the lamb heart was dissected. As can be seen from Fig. 2B, the hydrogel formed a self-contained, defined deposit at the injection site. This behaviour is consistent with the results above suggesting that the hydrogel upon injection does not become a low-viscosity liquid diffusing through the tissue, but instead breaks into micron-size domains which, upon leaving the needle tip, reassemble quickly into a well-defined, macroscopic hydrogel deposit. Interestingly, the pH of the hydrogel after injection was found to have changed (Fig. 2 inset) suggesting that diffusion of the heart extracellular fluid into the hydrogel occurred. This was confirmed by the hydrogel recovered after injection appearing stiffer. Indeed, as discussed above the diffusion of cell culture media, or any saline solution, into the hydrogel results in an increase in its G′ (Fig. ESI 1) [24].

Next, the hydrogel injectability was evaluated in vivo. As can be seen from Fig. 3A, the presence of a pink area corresponding to the site of injection in the left ventricular free wall was observed in formalin-fixed rat heart excised 7-days after injection of hydrogel loaded with rhodamine particles. In this case, to avoid extensive damage due to the actual procedure, the hydrogel was gently injected while the needle was retracted, resulting in the shown elongated injection site. No leakage of the hydrogel after fully removing the needle was observed, which is consistent with the rheological behaviour discussed above. The retention of rhodamine loaded hydrogel was further confirmed by examining a serial section of the heart injection site under UV light. Pink fluorescence corresponding to the rhodamine particles was clearly visible (Fig. 3B, right panel). This observation indicates that the hydrogel is indeed able to immobilise the rhodamine particles preventing them from being washed-out, opening the possibility of using the hydrogel not only to deliver cells but also for the topical delivery of drug-loaded microparticles. Histological analysis of serial sections of the heart stained with H&E and Masson's trichrome suggested a small localised immune response occurring at the injection site, together with a moderate deposition of collagen, commensurate with the response expected from the small injury caused by the needle (Fig. 3B, left and centre panels).

To confirm the presence of the hydrogel itself at the injection site and its ability to prevent cellular wash-out, an MCA labelled hydrogel was formulated and injected with and without QDot-stained CPCs in a healthy rat heart. Once again, the injection site was examined after 7-days, in this case using fluorescence microscopy. As shown in Fig. 3C, the hydrogel is still present and appears fragmented into domains of varying sizes, probably due to the injection procedure itself as well as to the beating of the heart. Indeed, both processes induce shear stresses that probably lead to the fragmentation of the hydrogel. After 7 days, QDot-labelled CPCs were still present confirming the ability of the hydrogel to retain cells at the injection site (Fig. 3C, lower panels).

In order to investigate the biocompatibility of the hydrogel and the effects of RGDSP-functionalisation, CPCs were encapsulated using a “sandwich” approach as illustrated in Fig. 4A. Briefly, a layer of hydrogel was plated and allowed to set, then a layer of cells and media was added on top, and finally an additional layer of hydrogel was deposited gently on top of the cells before adding cell culture media. As can be seen from Fig. 4B, after 6-days the CPCs cultured in FEFEFKFK hydrogel were found to remain viable, as shown by the presence of $EGFP^{pos}$ cells, and to migrate through gravity towards the bottom of the cell culture well. The morphology of the cells was found to change from round to flat and extended once the cells reached the bottom of the well, suggesting that the cells adhered to the cell culture plastic surface. The cells that were still fully embedded in the hydrogel were found to retain a rounded morphology. This behaviour suggests that the cells were not adhering the peptide fibrillar network. To improve cell-network interactions, a new functional hydrogel was formulated by incorporating 30% (wt.) of RGDSP-functionalised peptide. The optimal amount of RGDSP functionality to add was estimated through a simple 2D cell culture experiment using human dermal fibroblasts and examining their morphology (Fig. ESI 3). The addition of RGDSP functionalised peptide did not affect the mechanical properties of the hydrogel, nor its stability under cell culture condition (Fig. ESI 1). As can been seen from Fig. 4B, when RGDSP is added CPCs retained a round morphology and migrated in all directions throughout the hydrogel. Almost no settling to the bottom of the well was observed. This result suggests that the introduction of RGDSP promoted integrin binding of the cells to the fibrillar network, allowing them to migrate across the full volume of the functionalised hydrogel.

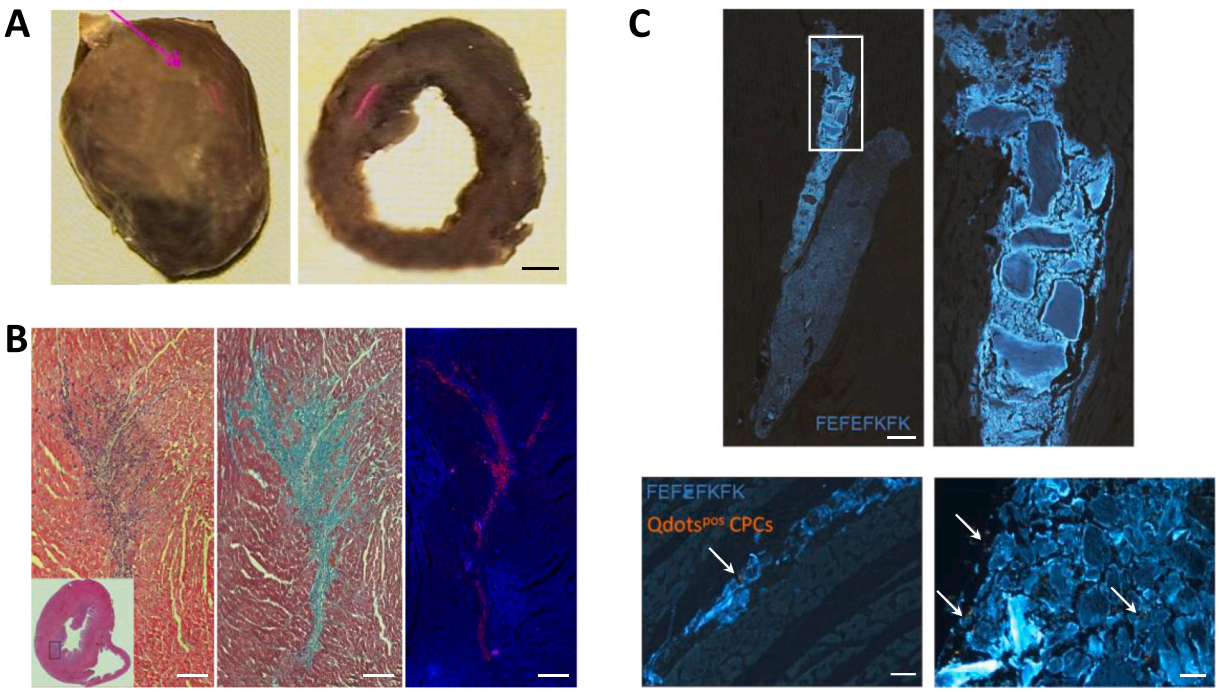

Fig. 3. A) Macro photograph of healthy rat heart LV free wall (left) and the corresponding equatorial cross section (right; scale bar: 1 mm) after injection of rhodamine particles (pink) loaded hydrogel; B) inset: equatorial section of an healthy rat heart (H&E) 7 days after injection of rhodamine particles loaded hydrogel (black rectangle indicates injection site. From left to right: higher magnification images of the same microscopic field showing the injection site on serial sections stained by H&E, Masson's trichrome and UV excited image showing the pink fluorescence of rhodamine particles (scale bars: 250 μm). C) Fluorescence images (UV light) of MCA labelled hydrogel (top; scale bar: 100 μm) and MCA labelled hydrogel loaded with QDot-labelled CPCs (bottom, arrows; scale bars: 25 μm) 7 days after injection in the LV rat heart. (For interpretation of the references to color in this figure legend, the reader is referred to the web version of this article.)

To examine the ability of the progenitor cells to differentiate towards cardiac lineages, CPCs cultured for 7 days in the hydrogels were extracted, re-plated and cultured for 2 weeks in standard 2D conditions. Differentiation towards cardiomyocytes and smooth muscle cells was evaluated through immunohistochemical analysis of α-SARC and α-SMA expression, respectively. Under standard conditions, typically CPC population consists of only 5% α-SMA and less than 1% α-SARC positive cells. As shown Fig. 4C, after 7-days of culture in both FEFEFKFK and RGDSP-FEFEFKFK hydrogels, CPCs were found to increase the expression of α-SARC and α-SMA. In particular, RGDSP-FEFEFKFK hydrogel induced a nearly 2-fold increase in the fractions of α-SMA positive cells compared to FEFEFKFK hydrogel; on the other hand, a ~1.4-fold increase in α-SARC positive CPCs was observed in FEFEFKFK hydrogel compared to RGDSP-FEFEFKFK hydrogel.

However, cardiomyocytes generated from CPCs encapsulated in the RGDSP-functionalised hydrogel were observed to have well-organized sarcomeric proteins (Fig. 4C), suggesting a more mature phenotype [47]. A similar observation was made in a recent study in which CPCs were encapsulated in RGDSP-functionalised PEG hydrogels, in which cells were found to upregulate cardiac structural proteins markers rather than cardiac lineage commitment markers [48]. The differentiation of CPCs after encapsulation in the hydrogels was also supported by the significantly lower growth rate observed during the 2D cell culture phase (Fig. ESI 2). The exact biological molecular mechanism leading to the differentiation of CPCs when cultured in these hydrogels is currently being investigated.

Two cardiac injury models were used for the purpose of this work: cryoinjury (CI), in which a frozen copper needle is pressed on the surface of the heart; and permanent ligation of the proximal left descending coronary artery. These two types of injuries result in very different cardiac damages, as can be seen from the histological sections in Fig. 5A (top panels). In CI, the damage was mainly localised to the pericardium where the needle was placed. After 10-days, additional collagen deposition was observed in areas distant from the original damage location, pointing towards remodelling of the myocardium due to irregular and aberrant wall stresses resulting from the original injury. For permanent ligation, after 30-days significant cardiac damage was observed that spanned the full thickness of the heart wall, consistent with MI. The difference in severity of cardiac damage led to different degrees of heart dilation, with left ventricle chamber volume increasing from 199 ± 11 mm^3 for a healthy rat heart [49] to 411 ± 17 mm^3 10-days after CI, a ~2-fold increase, and to 726 ± 50 mm^3 30-days after MI, a ~3.6-fold increase. These volume increases correlated with heart weight increases (Table ESI 1), pointing towards pathological cardiac hypertrophy.

Based on the in vitro results, we decided to use the RGDSP-functionalised hydrogel to deliver CPCs into rat hearts. Following injury, during the same surgical session, hydrogels with and without $EGFP^{pos}$ CPCs were injected into the peridamaged area of the hearts. In all cases, the injection of RGDSP-FEFEFKFK hydrogel, with or without CPCs, resulted in a significant reduction in collagen deposition across the heart (Fig. 5A lower panels) and a decrease in heart dilation after injury compared to the control groups (Fig. 5B), pointing towards a reduction in cardiac damage.

In the case of MI, no statistically significant differences in outcomes were observed between injection of hydrogel with and without CPCs after 30 days, in both cases a ~2 fold reduction in ventricular dilation was observed compared to the control group. The final left ventricle chamber volumes, 416 ± 17 mm^3 for hydrogel only and 350 ± 19 mm^3 for CPCs loaded RGDSP-functionalised hydrogel injection, were nevertheless still significantly higher compared to healthy rat heart, 1.8 to 2-fold increase. No $EGFP^{pos}$ cells could be observed 30 days after MI suggesting that they did not survive the significantly harsher MI environment, which may explain why the addition of CPCs did not result in any anatomical benefits.

In the case of CI, a statistically significant improvement was observed when loading the hydrogels with CPCs. At 10 days, a 1.6-fold reduction in ventricular dilation was observed when CPCs were added

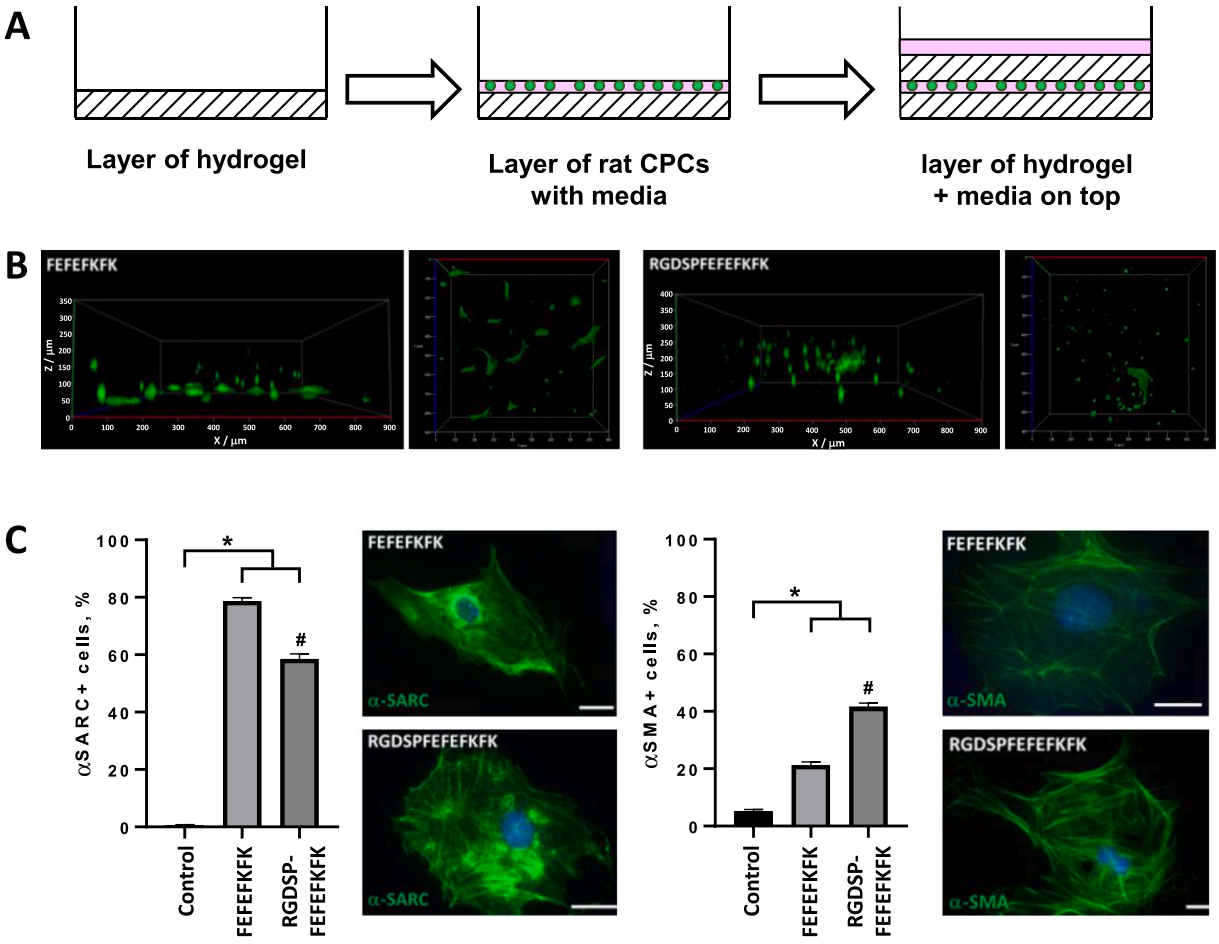

Fig. 4. A) Schematic representation of the "sandwich" encapsulation method used. B) 3D rendered confocal microscopy images showing distribution of $EGFP^{pos}$ CPCs (green fluorescence) in FEFEFKFK (left) and RGDSP-FEFEFKFK (right) hydrogels after 6 day of "sandwich" culture. C) Confocal images of wild type CPCs expressing α-SMA or α-SARC (green fluorescence) 2 weeks after rescue from FEFEFKFK or RGDSP-FEFEFKFK hydrogel "sandwich" culture (scale bars: 25 µm). Bar graphs document the ability of FEFEFKFK and RGDSP-FEFEFKFK hydrogel to induce differentiation of CPCs into cardiomyocytes (left) and smooth muscle cells (right) compared to the culture medium growth condition (Control). Results are expressed as Mean ± StDev (N = 3; *$p < 0.05$ versus Control; $^{\#}p < 0.05$ versus FEFEFKFK). (For interpretation of the references to color in this figure legend, the reader is referred to the web version of this article.)

compared to hydrogel only, with a left ventricle chamber volume, 208 ± 24 mm^3 (Table ESI 1), similar to the chamber volume of a healthy rat heart. In contrast, the absence of CPCs led to a chamber volume, 333 ± 26 mm^3, significantly larger compare to healthy rat heart, 1.7-fold increase. This result confirms the potential benefit of having CPCs delivered with the hydrogel in the CI model. Immunofluorescence analysis was performed to document progenitor cell homing and differentiation. Injected $EGFP^{pos}$ CPCs were detected at the injury site, both 4 and 10 days after CI (Fig. 5C). In particular, 10-days after CI, $EGFP^{pos}$ cells expressing α-SARC (Fig. 5C, inset) were found near the damaged myocardium suggesting CPCs not only survived, but also differentiated towards cardiomyocytes, thereby potentially explaining the beneficial effect of their delivery in the CI model.

The therapeutic effect of injecting hydrogel only is thought to be due to the procedure used for these experiments. Indeed, hydrogels were injected immediately after injury. It is well known that following MI tissue damage is not instantaneous and if early intervention occurs, for example coronary bypass, the long-term damage can be significantly reduced as cell death can be prevented by restoration of the blood flow. In our case, hydrogels are injected immediately after injury. When injecting hydrogels, several compounds that can improve cell survival are also injected, including salts, oxygen and amino acids resulting from the degradation of peptides. It is thought that this limits the damage resulting from the injury, leading to the reduced heart dilation observed. The addition of cells was beneficial only in the CI model after 10 days, in good agreement with the observation of CPCs differentiation towards cardiomyocytes.

4. Conclusion

In this work we have investigated the potential of using RGDSP-functionalised FEFEFKFK hydrogel as an injectable scaffold for the delivery and retention of progenitor cells into the injured rat heart. Our results clearly show that functionalising the hydrogel with RGDSP promotes migration of the cells across the material suggesting that cell adhesion to the peptide fibrillar network allows them to move through it. We also have shown that culturing CPCs within the hydrogel for one-week results in their spontaneous differentiation towards cardiac lineages. When injected in a CI model, the hydrogel was able to deliver the CPCs and retain them for up to 10 days at the injury site resulting in significantly reduced heart dilation, as measured through the left ventricle chamber volume. In the case of MI, cell presence was not observed after 30 days suggesting that CPCs may not survive the significant harsher condition resulting from MI compared to CI. Nevertheless, in all case injection of hydrogel only resulted in a reduction in heart damage.

CRediT authorship contribution statement

K. A. Burgess: Writing- Original draft preparation, Data curation

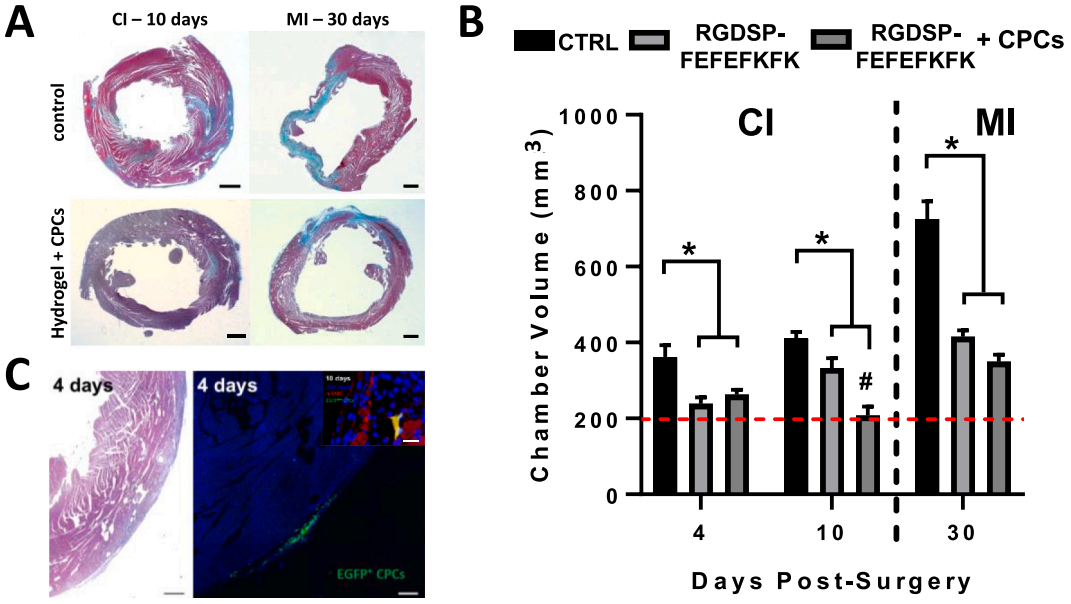

Fig. 5. A) Examples of LV cross sections of cryoinjured (CI) and myocardial infarcted (MI) rat hearts stained by Masson's trichrome from different experimental groups. (Scale bars: 1 mm). B) Bar graph showing left ventricular chamber volume in different experimental groups at 4 and 10 days for CI and 30 days for MI. Horizontal dotted red line indicates the average chamber volume of healthy Wistar rats. Results are presented as Mean ± StDev (raw data are presented in Table ESI 1; *p < 0.05 versus Control; #p < 0.05 versus FEFEFKFK). C) Serial sections of a rat heart 4 days after cryoinjury stained by Masson's trichrome (left panel; scale bars: 500 μm) and by immunofluorescence to detect $EGFP^{pos}$ CPCs (green florescence, right panel; scale bars: 25 μm). The right panel inset shows at high magnification a newly formed cardiomyocyte in yellow due to the co-expression of GFP (green) and α-SARC (red). (For interpretation of the references to color in this figure legend, the reader is referred to the web version of this article.)

C. Frati: Conceptualization, Validation, Methodology, Data curation
K. Meade: Conceptualization, Methodology, Validation, Data curation
J.Gao: Methodology, Data curation
L. Castillo Diaz: Methodology, Data curation
D. Madeddu: Methodology, Data curation
G. Graiani: Writing - reviewing and editing
S. Cavalli: Writing - reviewing and editing
A.F. Miller: Conceptualization, Writing - reviewing and editing
D. Oceandy: Writing - reviewing and editing
F. Quaini: Conceptualization, Writing - reviewing and editing, Supervision
Saiani: Conceptualization, Writing - original draft preparation, Writing - reviewing and editing, Supervision.

Declaration of competing interest

The authors declare that they have no known competing financial interests or personal relationships that could have appeared to influence the work reported in this paper.

Acknowledgements

The authors gratefully acknowledge funding from the European Union Framework Programme 7 (BIOSCENT Grant no.: 214539). AS also gratefully acknowledges funding from the UK Engineering and Physical Sciences Research Council (Fellowship Grant no.: EP/K016210/1). FQ acknowledges the support from the European Cooperation in Science and Technology (Action nº: 16122-BIONECA). DO acknowledges support from British Heart Foundation (Project Grant nPG/17/78/33304). All research data supporting this publication are directly available within this publication and associated Supporting information.

Appendix A. Supplementary data

Supplementary data to this article can be found online at https://doi.org/10.1016/j.msec.2020.111539.

References

[1] T.J. Cahill, R.K. Kharbanda, Heart failure after myocardial infarction in the era of primary percutaneous coronary intervention: mechanisms, incidence and identification of patients at risk, World J. Cardiol. 9 (5) (2017) 407–415.
[2] N. Conrad, A. Judge, J. Tran, H. Mohseni, D. Hedgecott, A.P. Crespillo, M. Allison, H. Hemingway, J.G. Cleland, J.J.V. McMurray, K. Rahimi, Temporal trends and patterns in heart failure incidence: a population-based study of 4 million individuals, Lancet 391 (10120) (2018) 572–580.
[3] O. Bergmann, S. Zdunek, A. Felker, M. Salehpour, K. Alkass, S. Bernard, S.L. Sjostrom, M. Szewczykowska, T. Jackowska, C. Dos Remedios, T. Malm, M. Andra, R. Jashari, J.R. Nyengaard, G. Possnert, S. Jovinge, H. Druid, J. Frisen, Dynamics of cell generation and turnover in the human heart, Cell 161 (7) (2015) 1566–1575.
[4] A.S. Bhatt, A.P. Ambrosy, E.J. Velazquez, Adverse remodeling and reverse remodeling after myocardial infarction, Curr. Cardiol. Rep. 19 (8) (2017) 71.
[5] J.N. Katz, S.B. Waters, I.B. Hollis, P.P. Chang, Advanced therapies for end-stage heart failure, Curr. Cardiol. Rev. 11 (1) (2015) 63–72.
[6] T.K. Rosengart, V. Patel, F.W. Sellke, Cardiac stem cell trials and the new world of cellular reprogramming: time to move on, J. Thorac. Cardiovasc. Surg. 155 (4) (2018) 1642–1646.
[7] T.K. Rosengart, E. Fallon, R.G. Crystal, Cardiac biointerventions whatever happened to stem cell and gene therapy? Innovations 7 (3) (2012) 173–179.
[8] P.A. Lalit, D.J. Hei, A.N. Raval, T.J. Kamp, Induced pluripotent stem cells for post-myocardial infarction repair: remarkable opportunities and challenges, Circ. Res. 114 (8) (2014) 1328–1345.
[9] S. Barreto, L. Hamel, T. Schiatti, Y. Yang, V. George, Cardiac progenitor cells from stem cells: learning from genetics and biomaterials, Cells 8 (12) (2019) 1536.
[10] V. Schwach, M. Gomes Fernandes, S. Maas, S. Gerhardt, R. Tsonaka, L. van der Weerd, R. Passier, C.L. Mummery, M.J. Birket, D.C.F. Salvatori, Expandable human cardiovascular progenitors from stem cells for regenerating mouse heart after myocardial infarction, Cardiovasc Res. 116 (2020) 545–553, https://doi.org/10.1093/cvr/cvz181.
[11] J. Cutts, M. Nikkhah, D.A. Brafman, Biomaterial approaches for stem cell-based myocardial tissue engineering, Biomark. Insights 10 (Suppl. 1) (2015) 77–90.
[12] D. He, A.-S. Zhao, H. Su, Y. Zhang, Y.-N. Wang, D. Luo, Y. Gao, J.-A. Li, P. Yang, An injectable scaffold based on temperature-responsive hydrogel and factor-loaded nanoparticles for application in vascularization in tissue engineering, J. Biomed. Mater. Res. A 107 (10) (2019) 2123–2134.
[13] Y. Ding, A.-s. Zhao, T. Liu, Y.-n. Wang, Y. Gao, J.-a. Li, P. Yang, An injectable

nanocomposite hydrogel for potential application of vascularization and tissue repair, Ann. Biomed. Eng. 48 (5) (2020) 1511–1523.
[14] O. Morris, M.A. Elsawy, M. Fairclough, K.J. Williams, A. McMahon, J. Grigg, D. Forster, A.F. Miller, A. Saiani, C. Prenant, In vivo characterisation of a therapeutically relevant self-assembling F-18-labelled -sheet forming peptide and its hydrogel using positron emission tomography, J. Labelled Comp. Radiopharm. 60 (10) (2017) 481–488.
[15] A. Markey, V.L. Workman, I.A. Bruce, T.J. Woolford, B. Derby, A.F. Miller, S.H. Cartmell, A. Saiani, Peptide hydrogel in vitro non-inflammatory potential, J. Pept. Sci. 23 (2) (2016) 148–154.
[16] F. Gelain, A. Horii, S.G. Zhang, Designer self-assembling peptide scaffolds for 3-D tissue cell cultures and regenerative medicine, Macromol. Biosci. 7 (5) (2007) 544–551.
[17] S. Koutsopoulos, Self-assembling peptide nanofiber hydrogels in tissue engineering and regenerative medicine: progress, design guidelines, and applications, J. Biomed. Mater. Res. (2016) 1002–1016.
[18] M.A. Elsawy, A.M. Smith, N. Hodson, A. Squires, A.F. Miller, A. Saiani, Modification of beta-sheet forming peptide hydrophobic face: effect on self-assembly and gelation, Langmuir 32 (19) (2016) 4917–4923.
[19] J. Gao, C. Tang, M.A. Elsawy, A.M. Smith, A.F. Miller, A. Saiani, Controlling self-assembling peptide hydrogel properties through network topology, Biomacromolecules 18 (3) (2017) 826–834.
[20] J.K. Wychowaniec, A.M. Smith, C. Ligorio, O.O. Mykhaylyk, A.F. Miller, A. Saiani, Role of sheet-edge interactions in β-sheet self-assembling peptide hydrogels, Biomacromolecules 21 (6) (2020) 2285–2297.
[21] D.M. Leite, E. Barbu, G.J. Pilkington, A. Lalatsa, Peptide self-assemblies for drug delivery, Curr. Top. Med. Chem. 15 (22) (2015) 2277–2289.
[22] W. Liyanage, K. Vats, A. Rajbhandary, D.S.W. Benoit, B.L. Nilsson, Multicomponent dipeptide hydrogels as extracellular matrix-mimetic scaffolds for cell culture applications, Chem. Commun. 51 (56) (2015) 11260–11263.
[23] R. Pugliese, F. Gelain, Peptidic biomaterials: from self-assembling to regenerative medicine, Trends Biotechnol. 35 (2017) 145–158, https://doi.org/10.1016/j.tibtech.2016.09.004.
[24] A. Mujeeb, A.F. Miller, A. Saiani, J.E. Gough, Self-assembled octapeptide scaffolds for in vitro chondrocyte culture, Acta Biomater. 9 (1) (2013) 4609–4617.
[25] L.A.C. Diaz, J. Gough, A. Saiani, A. Miller, Human osteoblasts within soft peptide hydrogels promote mineralisation in vitro, J. Tissue Eng. Regen. Med. 8 (2014) 159–160.
[26] L. Szkolar, J.B. Guilbaud, A.F. Miller, J.E. Gough, A. Saiani, Enzymatically triggered peptide hydrogels for 3D cell encapsulation and culture, J. Pept. Sci. 20 (7) (2014) 578–584.
[27] S.G. Zhang, T.C. Holmes, C.M. Dipersio, R.O. Hynes, X. Su, A. Rich, Self-complementary oligopeptide matrices support mammalian-cell attachment, Biomaterials 16 (18) (1995) 1385–1393.
[28] A. Faroni, V.L. Workman, A. Saiani, A.J. Reid, Self-assembling peptide hydrogel matrices improve the neurotrophic potential of human adipose-derived stem cells, Adv. Healthcare Mater. 8 (17) (2019) 1900410.
[29] D. Kumar, V.L. Workman, M. O'Brien, J. McLaren, L. White, K. Ragunath, F. Rose, A. Saiani, J.E. Gough, Peptide hydrogels-a tissue engineering strategy for the prevention of oesophageal strictures, Advanced Functional Materials 27 (38) (2017).
[30] C.E. Semino, J.R. Merok, G.G. Crane, G. Panagiotakos, S.G. Zhang, Functional differentiation of hepatocyte-like spheroid structures from putative liver progenitor cells in three-dimensional peptide scaffolds, Differentiation 71 (4–5) (2003) 262–270.
[31] M. Iwasaki, J.T. Wilcox, Y. Nishimura, K. Zweckberger, H. Suzuki, J. Wang, Y. Liu, S.K. Karadimas, M.G. Fehlings, Synergistic effects of self-assembling peptide and neural stem/progenitor cells to promote tissue repair and forelimb functional recovery in cervical spinal cord injury, Biomaterials 35 (2014) 2617–2629.
[32] Y. Luo, C. Lou, S. Zhang, Z. Zhu, Q. Xing, P. Wang, T. Liu, H. Liu, C. Li, W. Shi, Z. Du, Y. Gao, Three-dimensional hydrogel culture conditions promote the differentiation of human induced pluripotent stem cells into hepatocytes, Cytotherapy 20 (1) (2018) 95–107.
[33] M.R. Caplan, E.M. Schwartzfarb, S.G. Zhang, R.D. Kamm, D.A. Lauffenburger, Control of self-assembling oligopeptide matrix formation through systematic variation of amino acid sequence, Biomaterials 23 (1) (2002) 219–227.
[34] M.R. Caplan, P.N. Moore, S.G. Zhang, R.D. Kamm, D.A. Lauffenburger, Self-assembly of a beta-sheet protein governed by relief of electrostatic repulsion relative to van der Waals attraction, Biomacromolecules 1 (4) (2000) 627–631.
[35] M.R. Caplan, E.M. Schwartzfarb, S.G. Zhang, R.D. Kamm, D.A. Lauffenburger, Effects of systematic variation of amino acid sequence on the mechanical properties of a self-assembling, oligopeptide biomaterial, J. Biomater. Sci.-Polym. Ed. 13 (3) (2002) 225–236.
[36] S. Wan, S. Borland, S.M. Richardson, C.L.R. Merry, A. Saiani, J.E. Gough, Self-assembling peptide hydrogel for intervertebral disc tissue engineering, Acta Biomater. 46 (2016) 29–40.
[37] L.A.C. Diaz, M. Elsawy, A. Saiani, J.E. Gough, A.F. Miller, Osteogenic differentiation of human mesenchymal stem cells promotes mineralization within a biodegradable peptide hydrogel, J. Tissue Eng. 7 (2016) 2041731416649789.
[38] C.F. Guimarães, L. Gasperini, A.P. Marques, R.L. Reis, The stiffness of living tissues and its implications for tissue engineering, Nat. Rev. Mater. 5 (5) (2020) 351–370.
[39] E. Ruoslahti, RGD and other recognition sequences for integrins, Annu. Rev. Cell Dev. Biol. 12 (1996) 697–715.
[40] A. Horii, X.M. Wang, F. Gelain, S.G. Zhang, Biological designer self-assembling peptide nanofiber scaffolds significantly enhance osteoblast proliferation, differentiation and 3-D migration, PLoS One 2 (2) (2007) 9.
[41] K.M. Galler, L. Aulisa, K.R. Regan, R.N. D'Souza, J.D. Hartgerink, Self-assembling multidomain peptide hydrogels: designed susceptibility to enzymatic cleavage allows enhanced cell migration and spreading, J. Am. Chem. Soc. 132 (9) (2010) 3217–3223.
[42] N.J. Hogrebe, J.W. Reinhardt, N.K. Tram, A.C. Debski, G. Agarwal, M.A. Reilly, K.J. Gooch, Independent control of matrix adhesiveness and stiffness within a 3D self-assembling peptide hydrogel, Acta Biomater. 70 (2018) 110–119.
[43] M. Savi, L. Bocchi, S. Rossi, C. Frati, G. Graiani, C. Lagrasta, M. Miragoli, E.D. Pasquale, G.G. Stirparo, G. Mastrototaro, K. Urbanek, A.D. Angelis, E. Macchi, D. Stilli, F. Quaini, E. Musso, Antiarrhythmic effect of growth factor-supplemented cardiac progenitor cells in chronic infarcted heart, Am. J. Phys. Heart Circ. Phys. 310 (11) (2016) H1622–H1648.
[44] H.T. Dodge, W.A. Baxley, Left ventricular volume and mass and their significance in heart disease, Am. J. Cardiol. 23 (4) (1969) 528–537.
[45] C. Yan, A. Altunbas, T. Yucel, R.P. Nagarkar, J.P. Schneider, D.J. Pochan, Injectable solid hydrogel: mechanism of shear-thinning and immediate recovery of injectable β-hairpin peptide hydrogels, Soft Matter 6 (20) (2010) 5143–5156.
[46] S. Ramachandran, Y. Tseng, Y.B. Yu, Repeated rapid shear-responsiveness of peptide hydrogels with tunable shear modulus, Biomacromolecules 6 (3) (2005) 1316–1321.
[47] X.L. Yang, L. Pabon, C.E. Murry, Engineering adolescence maturation of human pluripotent stem cell-derived cardiomyocytes, Circ. Res. 114 (3) (2014) 511–523.
[48] S. Bhutani, A.L.Y. Nachlas, M.E. Brown, T. Pete, C.T. Johnson, A.J. García, M.E. Davis, Evaluation of hydrogels presenting extracellular matrix-derived adhesion peptides and encapsulating cardiac progenitor cells for cardiac repair, ACS Biomater. Sci. Eng. 4 (1) (2018) 200–210.
[49] L. Bocchi, M. Savi, G. Graiani, S. Rossi, A. Agnetti, F. Stillitano, C. Lagrasta, S. Baruffi, R. Berni, C. Frati, M. Vassalle, U. Squarcia, E. Cerbai, E. Macchi, D. Stilli, F. Quaini, E. Musso, Growth factor-induced mobilization of cardiac progenitor cells reduces the risk of arrhythmias, in a rat model of chronic myocardial infarction, PLoS One 6 (3) (2011) e17750.